High-power beam-based coherently enhanced THz radiation source

Yuelin Li (李跃林),[1] Yin-E Sun (孙银娥),[1,2] and Kwang-Je Kim[1]

[1]*Accelerator Systems Division and Argonne Accelerator Institute, Argonne National Laboratory, Argonne, Illinois 60439, USA*
[2]*Accelerator Physics Center, Fermi National Accelerator Laboratory, Batavia, Illinois 60510, USA*

(Received 10 March 2008; published 28 August 2008)

We propose a compact Smith-Purcell radiation device that can potentially generate high average power THz radiation with high conversion efficiency. The source is based on a train of short electron bunches from an rf photoemission gun at an energy of a few MeV. Particle tracking simulation and analysis show that, with a beam current of 1 mA, it is feasible to generate hundreds of watts of narrow-band THz radiation at a repetition rate of 1 MHz.

DOI: 10.1103/PhysRevSTAB.11.080701 PACS numbers: 07.57.Hm, 41.60.Cr, 29.27.Fh

Demand for terahertz radiation is increasing in many areas of science and technology, such as material characterization, chemical and biological analysis, and a variety of imaging applications [1]. Among various THz sources, laser-based techniques [2,3] and other compact sources [3] are limited to less than 1 W by the conversion efficiency and material damage threshold. A beam-based source can provide very high power of up to 1 kW but is normally based on large accelerator installations [4,5]. In this paper, we discuss a high power, efficient electron-beam-based source that is relatively compact.

The key for high efficiency in a beam-based radiation source, including free-electron lasers [4,5], is to exploit the coherence enhancement effect or quasiphase matching by beam profile tailoring. The radiation from an electron bunch consists of a coherent and an incoherent component [6]:

$$\frac{dI}{d\omega} = \left(\frac{d\boldsymbol{E}}{d\omega}\right)^2 [N + N^2\sigma_{\mathrm{coh}}], \tag{1}$$

where $d\boldsymbol{E}/d\omega$ and $dI/d\omega$ are, respectively, the radiation field from individual electrons and the spectral intensity from the bunch, and N is the total number of particles. Here σ_{coh} is effectively the normalized Fourier spectrum intensity,

$$\sigma_{\mathrm{coh}}(\omega) = \left[\frac{\int S(t)\cos(\omega t)dt}{\int S(t)dt}\right]^2, \tag{2}$$

with S being the particle distribution function. In Fig. 1, σ_{coh} is evaluated for a Gaussian distribution. Obviously, to harvest the coherent enhancement, i.e., the N^2 effect, an rms bunch length (σ_z) much smaller than the radiation wavelength (λ) is desired. In this case,radiation fields from individual particles are roughly in phase and add coherently. Such enhanced radiation due to short bunch length is the key in obtaining high radiation power in recent reports [4].

It is clear that higher charge per bunch is also desired. However, the charge that can be contained in a useful short bunch is limited by the space-charge force, proportional to Q/γ^2, where Q is the bunch charge and γ is the relativistic factor. The dynamics of such short bunches has been analyzed by several authors [7–9].

One way to reduce the space-charge force is to distribute the charge into evenly and resonantly spaced bunches. It follows that, for electron beams with repetitive temporal structure of $S(t - n\tau_b)$, $n = 1 \ldots N_b$, the overall coherence factor is

$$\Sigma_{\mathrm{coh}}(\omega) = \sigma_{\mathrm{coh}}(\omega)\frac{1}{N_b^2}\left[\frac{\sin\frac{N_b\tau_b}{2}\omega}{\sin\frac{\tau_b}{2}\omega}\right]^2, \tag{3}$$

where $\tau_b = 1/\beta c$ is the bunch spacing with β the particle speed normalized to the speed of light, and σ_{coh} is the single-bunch coherence factor in Eq. (2). The coherence factor at resonance, i.e., at $\omega = 2\pi/\tau_b$, is unaffected within a bandwidth of $1/N_b$. In another word, the radiation fields from individual bunches are phase matched to have a constructive superposition. This effect has been examined for the nonrelativistic bunch train [10] and was demonstrated for electron bunches spaced at ~1 cm for a Smith-

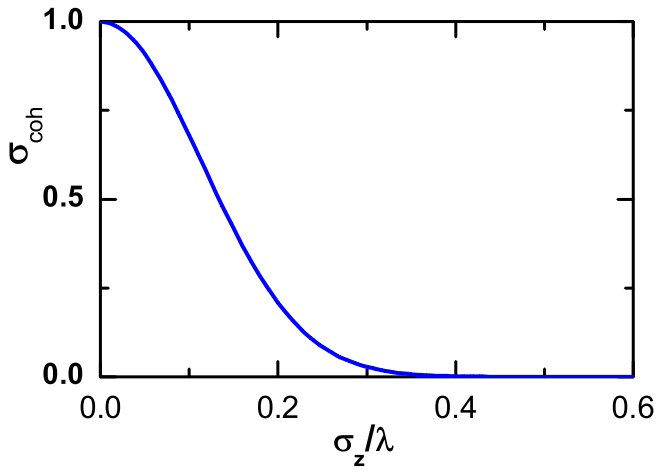

FIG. 1. (Color) Coherence factor as a function of the rms bunch length normalized to the radiation wavelength λ for a longitudinal Gaussian distribution.

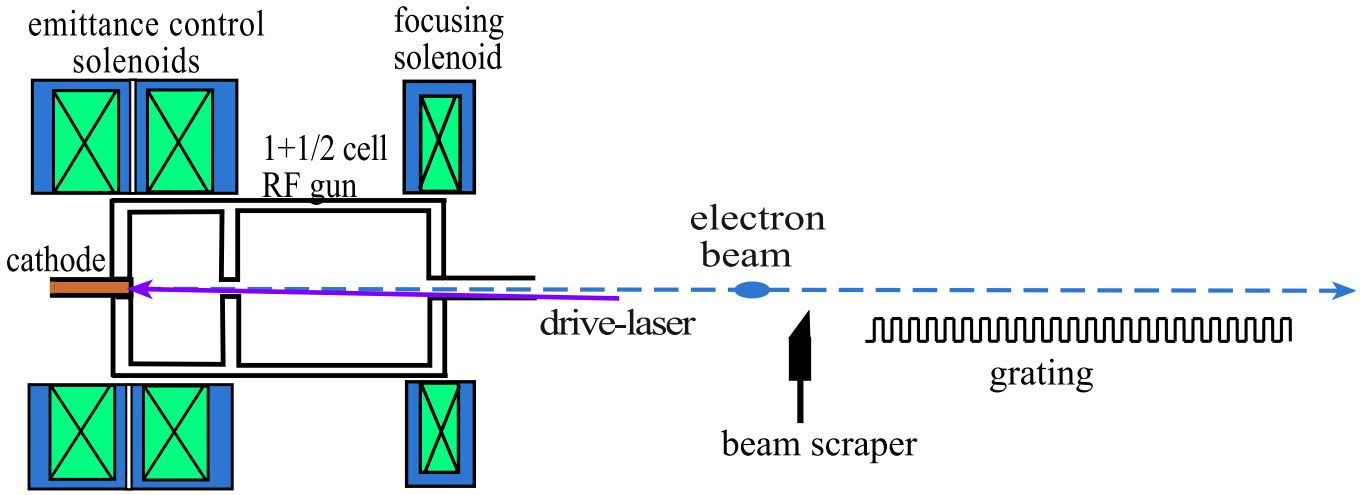

FIG. 2. (Color) Schematic of the proposed Smith-Purcell radiation scheme for high-power THz radiation source.

Purcell radiation (SPR) [11,12] experiment [13,14] and in a free-electron maser [15].

A further and more effective reduction of the space-charge force can be accomplished by increasing the beam energy, and in our example 8 MeV is considered. At this energy, the space-charge force is reduced by a factor of more than 200. Such a beam can be realized using a modern radiofrequency (rf) photoinjector driven by a laser system delivering pulse trains. A schematic of a feasible implementation is illustrated in Fig. 2, where a Smith-Purcell radiation scheme is considered.

Because of the complicated dynamics of the electron bunch in an rf photoinjector, we use numerical simulation to illustrate the evolution of the beams. We start by examining the single-bunch evolution in a photoemission gun at an rf of 1.3 GHz and accelerating gradient of 80 MV/m, using the code GPT [16]. A solenoid is used to focus the beam at about 0.6 m from the photocathode (see Fig. 2). Two-thousand particles are used for each electron bunch. The laser pulse has a longitudinal Gaussian (70 fs FWHM) and transverse top-hat (2-mm diameter) profile. The bunch-length evolution extracted from the particle tracking simulation is depicted in Fig. 3(a) for bunches with $Q =$ 31, 62, and 125 pC. As we can see, the bunch length σ_z displays a rapid increase within a few centimeters after being emitted from the cathode. This occurs due to the high space-charge force at low beam energy. As soon as the bunches acquire enough energy to enter the relativistic regime ($\gamma \gg 1$), the expansion slows significantly.

Figure 3(b) illustrates the evolution of the coherence factor for the corresponding cases in Fig. 3(a). Consider 0.5-THz radiation with $\lambda = 600$ μm. The $Q = 62.5$ pC bunch has a rms longitudinal bunch length $\sigma_z = 0.13\lambda$ at $z = 60$ cm from the cathode, and the corresponding co-

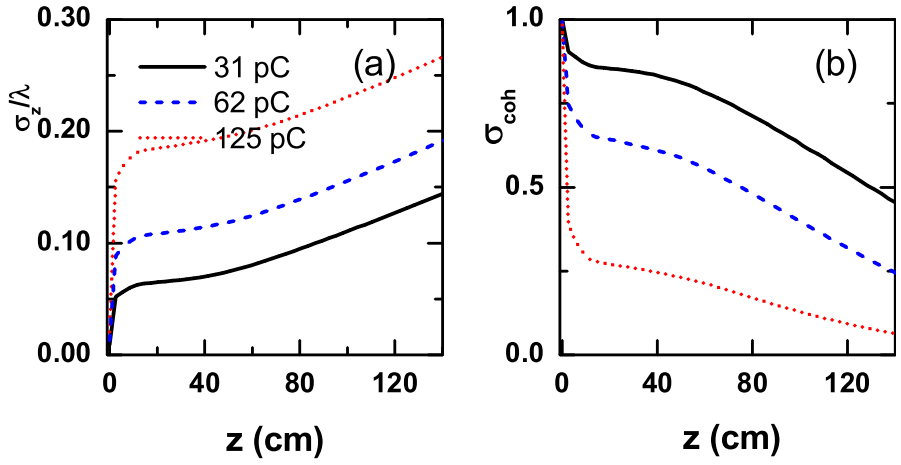

FIG. 3. (Color) (a) Evolution of the beam rms length normalized to the radiation wavelength and (b) evolution of the bunch coherence factor as a function of the bunch propagation distance for bunch charges $Q = 31$, 62, and 125 pC at $\lambda = 600$ μm (0.5 THz). The schematic is shown in Fig. 2 and is based on 80 MV/m peak accelerating gradient at 1.3 GHz rf.

herence factor is $\sigma_{coh} = 0.7$. Increasing Q to 125 pC, one has $\sigma_z = 0.2\lambda$ at $z = 60$ cm and $\sigma_{coh} = 0.3$. As the conversion efficiency is proportional to $Q^2\sigma_{coh}/Q \sim Q\sigma_{coh}$, this reduces the system efficiency slightly. Decreasing the bunch charge Q to 31 pC results in a coherence factor $\sigma_{coh} = 0.9$, leading also to a lower conversion efficiency. Obviously, there exists an optimum in conversion efficiency at around $Q = 62.5$ pC.

For the dynamics of the electron bunch train, we carried out a simulation using the code ASTRA [17] with 16 of the above bunches spaced at 2 ps, at resonance with 0.5-THz radiation. Figure 4(a) shows the phase space of the beam at $z = 60$ cm. The differences between the bunches are due to different rf phases they see during the emission and acceleration, as well as the interaction between the bunches. As expected from the result of the single-bunch evolution, the fidelity of individual bunches is well preserved.

The transverse profile and the spectrum of the bunch train averaged over the distance $z = 40$–76 cm are given in Figs. 4(b) and 4(c), respectively. The transverse beam profile can be fit nicely to a Lorentz distribution

$$f(x) = \frac{1}{\pi w}\frac{1}{1 + (\frac{x-h}{w})^2}. \quad (4)$$

Here $w = 200$ μm, and h is the distance from the beam center to the surface of the grating in the SPR scheme (see

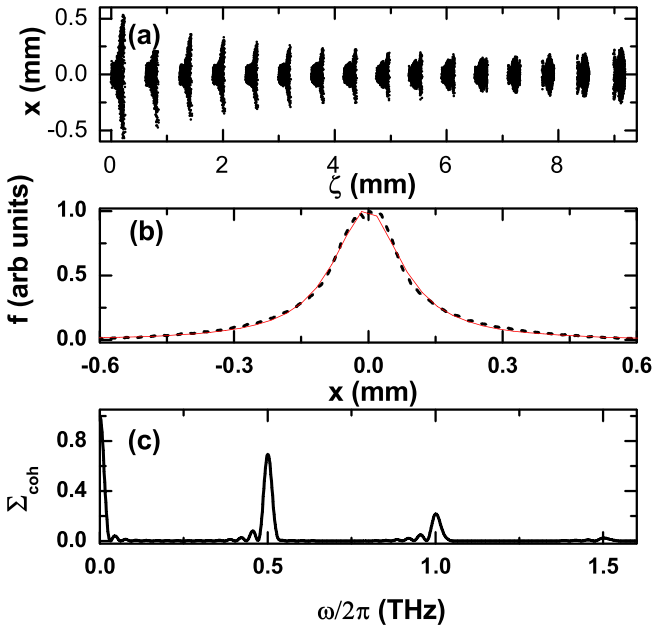

FIG. 4. (Color) (a) Particle distribution in the x-ζ plane, where $\zeta = z - vt$ with v the average particle speed and t the time, as seen by a screen at $z = 60$ cm. (b) The transverse beam profile (dashed) and the fitting to a Lorentz distribution with a 200-μm width (solid). (c) The normalized Fourier spectrum, i.e., the coherence factor Σ_{coh}, averaged over $z = 40$–70 cm. The total charge is 1 nC.

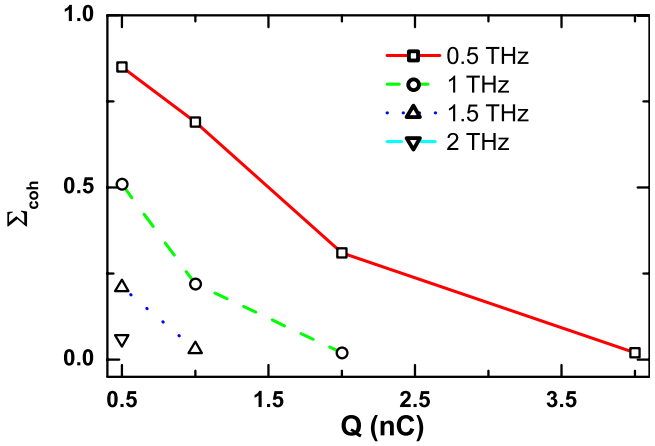

FIG. 5. (Color) Coherence factor at different radiation frequency as a function of the total beam charge.

Fig. 2). The normalized spectrum shows a coherence factor of 0.7 at 0.5 THz, and 0.2 at 1 THz, the second harmonic of the resonance frequency. The coherence factor as a function of the total bunch charge is shown in Fig. 5, showing the quick decrease of the coherence factor with increasing Q.

There are several well proved methods to generate the THz radiation, including bending magnet radiation, undulator radiation, or free-electron laser radiation, among others. Here the more compact Smith-Purcell radiation (SPR) scheme [11,12] is envisioned using a 20-cm-long grating centered at $z = 60$ cm with a period $\lambda_G = 600$ μm, thus a total number of periods is $N_G = 333$. SPR occurs when a charged particle passes close to a periodically varying metallic surface, forming a train of virtual dipoles. The radiation wavelength is a function of beam energy, the radiation angle θ, and the grating period,

$$\lambda = \frac{\lambda_G}{n}\left(\frac{1}{\beta} - \cos\theta\right), \quad (5)$$

where n is the diffraction order, and $\theta = 90°$ is measured from the grating surface. The radiation power of one electron is calculated as [12,13]

$$\frac{dI(x)}{d\omega} = \frac{e^2 N_G \lambda_G \omega \sin^2\theta}{8\pi^2\varepsilon_0 c^2}\int \Gamma \exp\left[-\frac{x}{\lambda_e}\right]\sin^2\phi\, d\phi, \quad (6)$$

where ϕ is the azimuthal angle, Γ is the grating efficiency, N_G is the total number of grating grooves, and x is the distance of the electron from the grating surface. The evanescent wavelength λ_e is defined as [12,13]

$$\lambda_e = \lambda\frac{\beta\gamma}{4\pi\sqrt{1 + \beta^2\lambda^2\sin^2\theta\sin^2\phi}}. \quad (7)$$

The total radiation power is thus estimated as

$$P = N^2\sigma_{coh}(\omega)\Delta\omega\int_{x=D}^{\infty}\frac{dI(x)}{d\omega}f(x)dx. \quad (8)$$

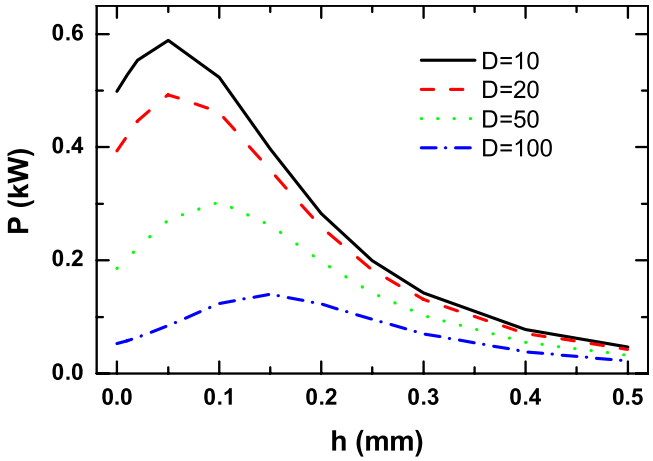

FIG. 6. (Color) Total radiation power as a function of the beam center-grating distance with a beam scraper height D in μm measured from the grating surface.

Here D is the height of a beam scraper in front of the grating (see Fig. 2) and $\Delta\omega = \omega/N_b$ is the bandwidth of the radiation. Using Eqs. (4)–(8), we evaluated the feasible performance of such a THz SPR source using the beam parameters with different setups regarding the height of the beam scraper (D) and the height of the beam from the grating (h). Figure 6 depicts the power as a function of beam center-grating surface distance h. The radiation power we arrive at ranges from 100 to 600 W within a bandwidth of $1/16$ at a repetition rate of 1 MHz: this is a conversion efficiency of 1% to 8% from the 8-kW beam power, several orders of magnitude higher than could be obtained from a nonrelativistic beam as discussed in Ref. [10].

We note that it is possible to use longer gratings to extract more radiation energy; however, one needs to match the grating shape to accommodate the change of the beam size. It should also be mentioned that, the radiation wavelength is determined by the beam velocity thus a beam energy loss due to radiation will lead to a shift of the radiation frequency. In our case, a radiation loss of 8% of beam energy at 8 MeV ($\gamma = 16$) only leads to a 0.04% change in velocity, from $\beta = 0.9980$ to $\beta = 0.9976$, with a negligible effect on frequency shift.

The above estimate is in good quantitative agreement with the detailed measurement of the coherent SPR radiation in Ref. [14], where 20 W of radiation at 0.12 GHz is measured for a 17 GHz pulse train, 4.67 pC per bunch at 15 MeV, with 20 grating periods. Using Eq. (1) and (5), by increasing the charge to 62.5 (corresponding to 1 nC in 16 bunches) and radiation frequency to 0.5 THz and the grating period number to 333, a radiation power of 300 kW is expected which corresponds to a conversion efficiency of 2% (taking into account the increase in beam power due to the increase of charge), already in the range of the 1% to 8% conversion efficiency estimated above. To reach the higher end of 8%, a tighter transverse beam distribution (0.2 mm in our case vs 1 mm in Ref. [14]) and a smaller beam-to-grating distance (less then 0.2 mm in our case and larger than 1 mm in Ref. [14]) should be considered.

With the conditions we assume, the radiation comes 90 degrees off the grating and can be collected using a collimating cylindrical mirror and further manipulated using more optics for delivery.

This scheme can be viewed as a SP THz free-electron laser seeded by the prebunched electron beam [15]. For such FEL action to grow from the beam noise, the requirement for the beam quality is practically difficult to achieve [18]. In comparison with a conventional FEL, the SPR scheme can be more compact. With further compression of the bunch and accelerating to higher beam energy, it is also possible to use this bunch for a much shorter radiation wavelength. We note a recent publication also simulates the evolution of a bunch train from a rf photoinjector at a high rf frequency [19] and experimental effort for generating beam structure modulation at long time scale [20].

There are several technical issues that need to be addressed to drive such a beam source. The first is the generation of the laser pulse train. This can be obtained using stacks of biaxial crystals with incremental thicknesses, as demonstrated in [21], where trains of up to 128 40-fs pulses at 800 nm were generated. For the example of 16 pulses spaced at 2 ps, a stack of 2, 4, 8, and 16 mm α-barium borate can be used and the group velocity dispersion in the crystal stack can be precompensated at the compressor of the laser system if needed. With an increasing number of bunches that can be accommodated by the rf, higher charge can be used, and the total radiation power increases quadratically as a function of the total charge.

The laser power for driving the necessary current of about 1 mA does not present a big obstacle. For cathode materials such as copper and magnesium, the response time is on the order of a few fs, and the quantum efficiency at 250 nm is between 5×10^{-5} to 5×10^{-4} [22,23]. With a 10% conversion efficiency from the fundamental to the third harmonic or fourth harmonic, a laser at 1 μm of less than 100 W is enough to drive the gun to produce the required beam current. Both the required power and comparable pulse duration have already been achieved by current fiber laser technology at the desired high repetition rate [24–26]. For example, in Ref. [26], 63 fs pulses at 1 μm are generated using a Yb doped fiber chirped pulse amplification system with 0.29 μJ per pulse at 27 MHz, a power of 8 W; and there is no obstacle to push for 1 μJ per pulse at the same peak power level and higher repetition rate for higher average power [26], such as the 220 fs pulses at 77 MHz with 130 W in Ref. [24]. With high repetition rate systems, a lossless cavity can be used to bring down the rate to 1 MHz with no pulse distortion [27].

Finally, rf guns at a repetition rate of 1 MHz or higher, the most challenging component in the system, are under

development at several laboratories either using superconductor or normal conductor technology [28,29]. However, the proper accelerating gradient of 80 MV/m at 1300 MHz and total current of larger than the benchmark number of 1 mA has been demonstrated [28,29].

In summary, we propose to generate a relativistic bunch train in an rf photoemission gun for a compact THz radiation source that is able to deliver hundreds of watts of radiation power in a relatively compact setup. The scheme can also be applied for a THz free-electron laser for even higher radiation power and can also serve as a prebuncher in a short wavelength free-electron laser in, e.g., a harmonic cascade scheme for a more efficient system [30].

ACKNOWLEDGMENTS

The authors thank K. Harkay for support. This work is supported by the U.S. Department of Energy, Office of Science, Office of Basic Energy Sciences, under Contract No. DE-AC02-06CH11357.

[1] B. Ferguson and X. C. Zhang, Nature Mater. **1**, 26 (2002).
[2] K. Kawase, J. Shikata, K. Imai, and H. Ito, Appl. Phys. Lett. **78**, 2819 (2001).
[3] See, for example, D. Abbott and X.-C Zhang, Proc. IEEE **95**, 1509 (2007), and references therein.
[4] G. L. Carr, M. C. Martin, W. R. McKinney, K. Jordan, G. R. Neil, and G. P. Williams, Nature (London) **420**, 153 (2002).
[5] S. V. Miginsky, N. A. Vinokurov, D. A. Kayran, B. A. Knyazev, E. I. Kolobanov, V. V. Kotenkov, V. V. Kubarev, G. N. Kulipanov, A. V. Kuzmin, A. S. Lakhtychkin, A. N. Matveenko, L. E. Medvedev, L. A. Mironenko, A. D. Oreshkov, V. K. Ovchar, V. M. Popik, T. V. Salikova, S. S. Serednyakov, A. N. Skrinsky, O. A. Shevchenko, and M. A. Scheglov, in Proceedings of the 2007 Asian Particle Accelerator Conference, Indore, India, Raja Ramanna Centre for Advanced Technology (RRCAT), p. 661, http://accelconf.web.cern.ch/AccelConf/a07/PAPERS/THC3MA04.PDF.
[6] J. S. Nodvick and D. S. Saxon, Phys. Rev. **96**, 180 (1954).
[7] Y. K. Batygin, Phys. Plasmas **8**, 3103 (2001).
[8] B. J. Siwick, J. R. Dwyer, R. E. Jordan, and R. J. D. Miller, J. Appl. Phys. **92**, 1643 (2002).
[9] A. M. Michalik and J. E. Sipe, J. Appl. Phys. **99**, 054908 (2006).
[10] Y. Li and K.-J. Kim, Appl. Phys. Lett. **92**, 014101 (2008).
[11] S. J. Smith and E. M. Purcell, Phys. Rev. **92**, 1069 (1953).
[12] P. M. van den Berg, J. Opt. Soc. Am. **63**, 1588 (1973).
[13] S. E. Korbly, A. S. Kesar, J. R. Sirigiri, and R. J. Temkin, Phys. Rev. Lett. **94**, 054803 (2005).
[14] S. Kesar, R. A. March, and R. J. Temkin, Phys. Rev. ST Accel. Beams **9**, 022801 (2006).
[15] M. Arbel, A. Abramovich, A. L. Eichenbaum, A. Gover, H. Kleinman, Y. Pinhasi, and I. M. Yakover, Phys. Rev. Lett. **86**, 2561 (2001), and references therein.
[16] http://www.pulsar.nl/gpt.
[17] http://tesla.desy.de/~lfroehli/astra/.
[18] H. L. Andrews and C. A. Brau, Phys. Rev. ST Accel. Beams **7**, 070701 (2004).
[19] M. Boscolo, M. Ferrario, I. Boscolo, F. Castelli, and S. Cialdi, Nucl. Instrum. Methods Phys. Res., Sect. A **577**, 409 (2007).
[20] J. G. Neumann, P. G. O'Shea, D. Demske, W. S. Graves, B. Sheehy, H. Loos, and G. L. Carr, Nucl. Instrum. Methods Phys. Res., Sect. A **507**, 498 (2003).
[21] B. Dromey, M. Zepf, M. Landreman, K. O'Keeffe, T. Robinson, and S. M. Hooker, Appl. Opt. **46**, 5142 (2007).
[22] D. H. Dowell, F. K. King, R. E. Kirby, J. F. Schmerge, and J. M. Smedley, Phys. Rev. ST Accel. Beams **9**, 063502 (2006).
[23] T. Srinivasan-Rao, I. Ben-Zvi, J. Smedley, X. J. Wang, and M. Woodle, in *Proceedings of the Particle Accelerator Conference, Vancouver, BC, Canada, 1997* (IEEE, New York, 1998), p. 2790.
[24] F. Röser, J. Rothhard, B. Ortac, A. Liem, O. Schmidt, T. Schreiber, J. Limpert, and A. Tünnermann, Opt. Lett. **30**, 2754 (2005).
[25] P. Dupriez, C. Finot, A. Malinowski, J. K. Sahu, J. Nilsson, D. J. Richardson, K. G. Wilcox, H. D. Foreman, and A. C. Tropper, Opt. Express **14**, 9611 (2006).
[26] D. N. Papadopoulos, Y. Zaouter, M. Hanna, F. Druon, E. Mottay, E. Cormier, and P. Georges, Opt. Lett. **32**, 2520 (2007).
[27] R. Jason Jones and Jun Ye, Opt. Lett. **27**, 1848 (2002).
[28] D. H. Dowell, J. W. Lewellen, D. Nguyen, and R. Rimmer, Nucl. Instrum. Methods Phys. Res., Sect. A **557**, 61 (2006).
[29] A. Todd, Nucl. Instrum. Methods Phys. Res., Sect. A **557**, 36 (2006).
[30] M. Cornacchia, S. Di Mitri, G. Penco, and A. A. Zholents, Phys. Rev. ST Accel. Beams **9**, 120701 (2006), and references therein.